



Research paper

Structure and magnetic properties of trinuclear copper(II) complex $[\text{Cu}_3(\text{bipy})_6(\mu^3\text{-CO}_3)][\text{B}_{12}\text{H}_{12}]_2 \cdot 4.5\text{DMF} \cdot 2\text{H}_2\text{O}$



Elena A. Malinina, Irina K. Kochneva, Irina N. Polyakova, Varvara V. Avdeeva*, Grigorii A. Buzanov, Nikolai N. Efimov, Elena A. Ugolkova, Vadim V. Minin, Nikolai T. Kuznetsov

Kurnakov Institute of General and Inorganic Chemistry, Russian Academy of Sciences, Leninskii Pr. 31, Moscow 119991, Russia

ARTICLE INFO

Article history:

Received 23 March 2018
 Received in revised form 25 April 2018
 Accepted 26 April 2018
 Available online 3 May 2018

ABSTRACT

Trinuclear copper(II) complex $[\text{Cu}_3^{\text{II}}(\text{bipy})_6(\mu^3\text{-CO}_3)][\text{B}_{12}\text{H}_{12}]_2 \cdot 4.5\text{DMF} \cdot 2\text{H}_2\text{O}$ is isolated as a result of the redox reaction proceeding when $[\text{Ag}_2\text{B}_{12}\text{H}_{12}]$ was allowed to react with $\text{Cu}^{\text{I}}\text{Cl}$ in the presence of bipy. Crystal structure, magnetic properties, and EPR spectrum of the compound are studied. It has been found that in the range 300–2 K, magnetic moment decreases from 1.98 to 1.33 μ_{B} with decreasing the temperature. In the EPR spectrum, the transition $\Delta M = \pm 3$ transition is observed indicating the existence of the $S = 3/2$ state. This transition is explained by the effect of fine coupling tensor which admixes the $| -1 \rangle$ state into the $| 3/2 \rangle$ state and the $| 1/2 \rangle$ state into the $| -3/2 \rangle$ state. The EPR spectrum is simulated by the spin Hamiltonians for $S = 3/2$ and $S = 1/2$.

© 2018 Elsevier B.V. All rights reserved.

1. Introduction

Design of substances with desired properties sets a task of synthesizing coordination compounds of new structural types. Homo- and heterometallic polynuclear transition metal complexes attract interest as potential molecular magnets and models of magnetic interactions between metal atoms. A great number of these compounds are present in Cambridge Structural Database and magnetic properties are reported in many studies indicating crucial interest in this type of compounds.

Here, we have studied the reaction ability of the dodecahydro-closo-dodecaborate anion $[\text{B}_{12}\text{H}_{12}]^{2-}$ in copper complexation. In coordination chemistry, boron cluster anions $[\text{B}_n\text{H}_n]^{2-}$ ($n = 10, 12$) [1,2] can be regarded as soft bases; they can act as inner-sphere ligands in copper(I), silver(I), and lead(II) complexes (with soft acid metals) [3,4] and form anionic parts of cationic 3d metal complexes [5]. Our long-term studies on the reaction ability of boron cluster anions $[\text{B}_n\text{H}_n]^{2-}$ ($n = 10, 12$) in complexation reaction showed that these compounds can result in interesting products because of reactions accompanied metal complexation. In particular, redox processes were observed in the course of iron(III) and cobalt(III) complexation which are discussed in details in the review [5].

A great number of copper complexes in various oxidation states (copper(I), copper(II), heterovalent copper(I,II) compounds) were

prepared for boron clusters and azaheterocyclic ligands 2,2'-bipyridyl, 2,2'-bipyridylamine, 1,10-phenanthroline, phenanthridine. Many of them are reported in our review [3]. Among them, mononuclear, binuclear, and polynuclear copper(II) cationic complexes were found to form with boron cluster anions usually acting as counterions. For bipy, tetranuclear copper(II) complex $[\text{Cu}_4^{\text{II}}(\text{bipy})_4(\text{OH})_4][\text{B}_{10}\text{H}_{10}]_2(\text{DMSO})_2$ [6] and binuclear copper(II) complex $[\text{Cu}_2^{\text{II}}(\text{phen})_4(\text{CO}_3)][\text{B}_{10}\text{H}_{10}]$ [7,8] as well as heterovalent copper(I,II) complex $[\text{Cu}_4^{\text{II}}(\text{bipy})_4(\text{OH})_4][\text{Cu}_2^{\text{I}}[\text{B}_{10}\text{H}_{10}]_3]$ [9] containing the mentioned tetranuclear copper(II) cationic complex were obtained for the $[\text{B}_{10}\text{H}_{10}]^{2-}$ anion in copper(I) complexation reactions including copper(I) oxidation in the $[\text{Cu}_2^{\text{I}}[\text{B}_{10}\text{H}_{10}]]/\text{L}$ systems ($\text{L} = \text{bipy}, \text{phen}$). Mononuclear [10], binuclear [11], tetranuclear [10], and polynuclear [10] copper(II) complexes were selectively prepared and studied by X-ray diffraction for phen whereas only a binuclear copper(II) complex with CO_3 bridged ligands was synthesized for bipy $[\text{Cu}_2^{\text{II}}(\text{bipy})_4(\text{CO}_3)][\text{B}_{10}\text{H}_{10}]$ as $\text{DMF}/\text{H}_2\text{O}$ and CH_3CN solvates [11]. The majority of copper(II) compounds were prepared starting from copper(I) salts in air as a result of copper(I) oxidation.

In this paper, we report the synthesis, structure, and magnetic properties of copper(II) complex $[\text{Cu}_3^{\text{II}}(\text{bipy})_6(\mu^3\text{-CO}_3)][\text{B}_{12}\text{H}_{12}]_2 \cdot 4.5\text{DMF} \cdot 2\text{H}_2\text{O}$ prepared when using copper(I) chloride as starting reagent. This compound is the first trinuclear copper(II) complex with boron cluster anions; it contains the bridging $\mu^3\text{-CO}_3$ group, terminal bipy molecules, and the dodecahydro-closo-dodecaborate anion as a counter ion.

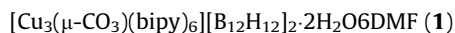
* Corresponding author.

E-mail address: avdeeva.varvara@mail.ru (V.V. Avdeeva).

2. Experimental

2.1. Synthesis

DMF (HPLC grade) and anhydrous Bipy and CuCl were purchased from Aldrich. $(\text{Et}_3\text{NH})_2[\text{B}_{12}\text{H}_{12}]$ was synthesized from decaborane-14 according to the known procedure [12]. $[\text{Ag}_2[\text{B}_{12}\text{H}_{12}]]$ was prepared from $(\text{Et}_3\text{NH})_2[\text{B}_{12}\text{H}_{12}]$ as indicated in [13].



A solution of CuCl (0.4 mmol) in DMF (10 ml) was added to a solution of $[\text{Ag}_2[\text{B}_{12}\text{H}_{12}]]$ (0.2 mmol) in DMF (10 ml) followed by the addition of a solution of bipy (0.8 mmol) in acetonitrile (10 ml). Once bipy was added, the reaction solution became red and changed its color to blue for seconds because of copper oxidation in air. Metallic silver precipitated as black powder for 1–2 h, which was filtered off. Blue crystals **1** precipitated for 72 h from the mother solution; which were filtered off, washed with acetonitrile, and dried in air. Yield, 30%. Anal. Calcd. %: Cu, 12.96; C, 49.79; H, 4.93; N, 11.42; B, 17.63. Found: Cu, 12.98; C, 49.76; H, 4.92; N, 11.44; B, 17.65.

2.2. Materials and methods

Elemental analysis for carbon, hydrogen, and nitrogen was carried out on a Carlo Erba CHNS-3 FA 1108 automated elemental analyzer. Determination of boron and metals was performed on an iCAP 6300 Duo ICP emission spectrometer with inductively coupled plasma. The samples were dried under vacuum at room temperature to constant weight to obtain solvent-free compounds.

IR spectrum of the crystals obtained was recorded on a Lumex Infracal FT-02 Fourier-transform spectrophotometer in the range of 4000–600 cm^{-1} at a resolution of 1 cm^{-1} . The sample was prepared as a CCl_4 mull; NaCl pellets were used. The IR spectrum of compound **2** is present in Fig. S1 (see SI).

The electronic structure of compound **1** was studied by EPR at $T = 295$ K. The EPR spectrum of the polycrystalline sample was recorded on a Bruker ELEXSYS E680X X band (frequency, 9.8 GHz) spectrometer. The spin Hamiltonian parameters were determined by means of computer simulation through fitting the theoretical spectra to the experimental ones [14].

The DC magnetic susceptibility of polycrystalline sample **1** was measured in the temperature range 300–2 K at 500 mT using a Quantum Design susceptometer PPMS-9.

2.3. X-ray diffraction

Experimental data were collected on a Bruker SMART APEX II diffractometer using graphite monochromatized MoK_α -radiation ($\lambda = 0.71073$ Å) in ω -scan mode. Absorption correction based on measurements of equivalent reflections were applied (SADABS

software; Bruker 2008). The structure was solved by direct methods and refined by full matrix least-squares on F^2 [15] with anisotropic thermal parameters for all non-hydrogen atoms except minor components of disordered groups. Both bipy ligands around Cu(1) atom were found to be positionally disordered over two positions with occupancy ratio 0.75/0.25. The minor parts of these disordered ligands were refined with restrained C–C and C–N distances. Two of five solvent DMF molecules were also disordered over two positions. They were refined with restrained C–N and C–O bond lengths. All hydrogen atoms were placed in calculated positions and refined using a riding model. The crystallographic data and experimental details are collected in Table S2; bond lengths and bond angles are listed in Table S3 (see SI).

The crystallographic data for **1** has been deposited with the Cambridge Crystallographic Data Centre as supplementary publications under the CCDC number 1559297. This information may be obtained free of charge from the Cambridge Crystallographic Data Centre via www.ccdc.cam.ac.uk/data_request/cif.

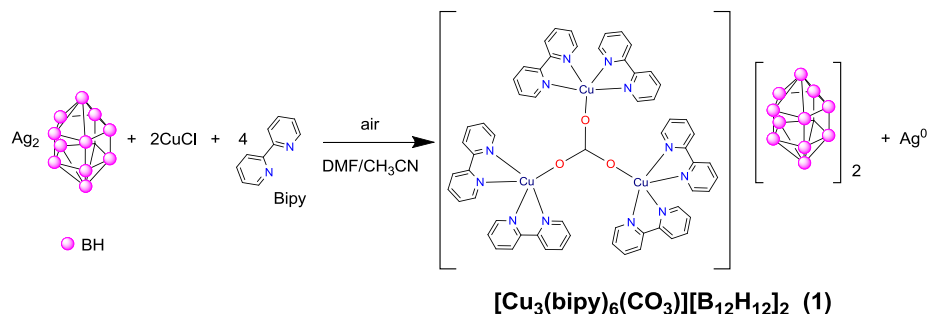
The X-ray powder diffraction pattern of complex **1** was measured on a Bruker D8 Advance diffractometer ($\text{CuK}_{\alpha 1}$) at RT with LynxEye detector and Ge(111) monochromator, $\theta/2\theta$ scan from 5° to 80° , step size 0.01125° at the Shared Equipment Centre of the Kurnakov Institute. The measurement was performed in transmission mode with the sample deposited in the single-crystal oriented silicon cuvette. The crystals were thoroughly triturated before measurements. The X-ray powder diffraction pattern for **1** is shown in Fig. S2 (see SI).

3. Results and discussion

Trinuclear copper complex $[\text{Cu}_3(\text{bipy})_6(\mu^3\text{-CO}_3)][\text{B}_{12}\text{H}_{12}]_2 \cdot 4.5\text{DMF} \cdot 2\text{H}_2\text{O}$ (**1**) was isolated as the main product of the reaction proceeding in the $[\text{Ag}_2[\text{B}_{12}\text{H}_{12}]]/\text{CuCl}/\text{bipy}$ system in a DMF/ CH_3CN solution. The reduction of silver(I) to metallic silver $\text{Ag}^+ \rightarrow \text{Ag}^0$ occurs along with the oxidation of copper(I) to copper(II) $\text{Cu}^+ \rightarrow \text{Cu}^{2+}$ as shown in Scheme 1.

The presence of the CO_3^{2-} group in the final compound is explained by air CO_2 and its dissolution in DMF, since the reaction was carried out in air. Previously, carbonate group was found in a number of copper(II) complexes with phen and bipy and anions $[\text{B}_n\text{H}_n]^{2-}$ ($n = 10, 12$) [7,8,11].

The composition of the complex was determined by elemental analysis and the purity of the product was proved by X-ray powder diffraction (Fig. S1). In the IR spectrum of a suspension of **1** in CCl_4 (Fig. S2), the stretching vibrations of the BH groups $\nu(\text{BH})$ appear as an intense broadened band with the maximum at 2467 cm^{-1} . The $\nu(\text{C}=\text{O})$ band of the bridging CO_3 group is observed at ~ 1400 cm^{-1} ; the sample was studied as a CCl_4 suspension to reveal the presence of the $(\text{C}=\text{O})$ band, which is overlaid by the $\delta(\text{HCH})$ bands when the sample is used as Nujol mull. The set of absorption bands of bipy molecules appears in the range 1600 – 800 cm^{-1} . The bands



Scheme 1. Preparation of compound **1**.

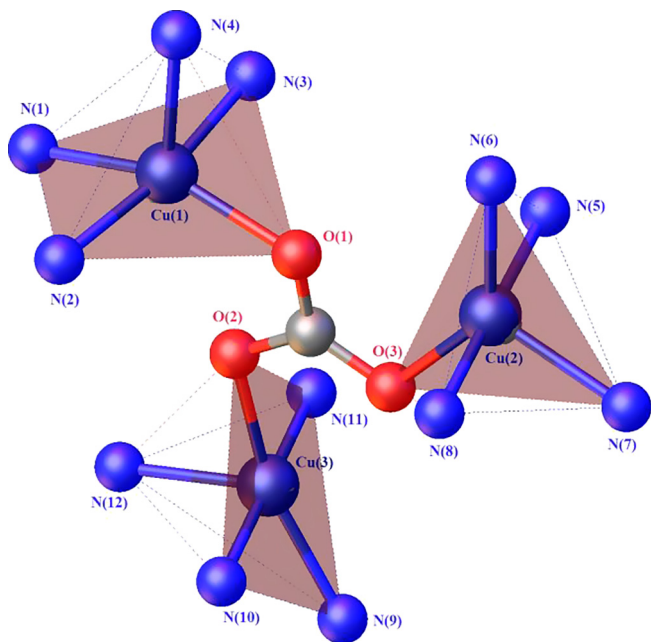


Fig. 1. Structure of the coordination nodes of the $[\text{Cu}_3(\text{bipy})_6(\mu_3\text{-CO}_3)]^{4+}$ complex cation.

with maxima at 1680 and 3450 cm^{-1} are attributed to the $\nu(\text{C}=\text{O})$ and $\nu(\text{OH})$ vibrations of solvate DMF and water molecules, respectively.

The crystal structure of $[\text{Cu}_3(\text{bipy})_6(\mu_3\text{-CO}_3)][\text{B}_{12}\text{H}_{12}]_2 \cdot 4.5\text{DMF} \cdot 2\text{H}_2\text{O}$ is built of trinuclear cations, $[\text{B}_{12}\text{H}_{12}]^{2-}$ anions, and solvate molecules of DMF and water (Fig. S3). The bridging carbonate anion is bound to Cu atoms by the $\mu_3\text{-}\eta^1\eta^1\eta^1$ pattern (Fig. 1). The $\text{Cu}_3(\text{CO}_3)$ core of the cation is flattened (Fig. S4): the Cu(1) and Cu(2) atoms deviate unidirectionally from the plane of the CO_3 group by 0.293 and 0.111 Å, and the Cu(3) atom deviates to the opposite direction by 0.105 Å. The cation has the *syn-anti* configuration in relation to all C–O bonds. The Cu...Cu distances in the trinuclear cation are 4.663, 4.666, and 4.888 Å.

The five-coordinate environment of the Cu(1), Cu(2), and Cu(3) atoms in the cation consists of four N atoms of bipy molecules and an O atom of the carbonate group (Fig. S5). The ranges of interatomic distances are as follows: Cu–O, 2.015(8)–2.119(9) Å; Cu(1)–N, 2.009(1)–2.126(8); Cu(2)–N, 1.969(8)–2.104(7); and Cu(3)–N, 1.991(7)–2.155(8) Å. The shapes of distorted polyhedra of the Cu(1) and Cu(3) atoms are close to the elongated square pyramids with the N(4) and N(12) atoms, respectively, at the apical vertices. The polyhedron of the Cu(2) atom is approximated by the slightly oblate trigonal bipyramid with the N(5) and N(8) atoms at the apical vertices (Fig. 1).

In the crystal structure, complex cations $\{[\text{Cu}(\text{bipy})_2]_3(\mu_3\text{-CO}_3)\}^{4+}$ are packed into columns running along the *b* axis (Figs. S6). Columns related by the *a* translation form loose layers separated by wide interlayer space filled by $[\text{B}_{12}\text{H}_{12}]^{2-}$ anions and solvate DMF and water molecules (Figs. S7). The geometric parameters of the C–H...O and O–H...O hydrogen bonds found in the structure of complex **1** are listed in Table S1; fragments showing the interactions are shown in Fig. S8.

Two crystallographically independent $[\text{B}_{12}\text{H}_{12}]^{2-}$ anions form multiple weak B–H...H–X (X=C, O) interactions with complex cations and solvate molecules: one of them has 12 contacts of 2.16–2.41 Å with bipy ligands and 3 contacts of 2.15–2.32 Å with DMF molecules, and the other has 5 contacts of 2.23–2.43 Å with bipy and 6 contacts of 2.26–2.44 Å with DMF and H_2O molecules.

The Cambridge Database (CSD version 5.37, November 2015) [16] contains data on six solvates that include trimeric $[(\text{Cu}(\text{bipy})_2)_3\text{CO}_3]^{4+}$ cation (Cat): Cat(BF_4) $_4 \cdot \text{EtOH} \cdot 3\text{H}_2\text{O}$ [17], Cat(ClO_4) $_4 \cdot 0.5\text{H}_2\text{O}$ [18], Cat(ClO_4) $_4 \cdot 4\text{EtOH} \cdot 2\text{H}_2\text{O}$ [19], Cat(F_3CSO_3) $_4 \cdot 0.5\text{H}_2\text{O}$ [20], Cat(ClO_4) $_4 \cdot \text{MeOH} \cdot 2\text{H}_2\text{O}$ [19], and Cat(PF_6) $_4 \cdot \text{H}_2\text{O}$ [19]. In the two latter compounds, the carbonate ligand is bound to copper atoms by the $\mu_3\text{-}\eta^2\eta^2\eta^2$ and $\mu_3\text{-}\eta^2\eta^1\eta^1$ patterns, respectively. In the remaining four trinuclear compounds, the coordination pattern is the same as in **1** and the shapes of CuON_4 five-vertex polyhedra are also better approximated by two square pyramids and a trigonal bipyramid. In the square pyramids, the Cu– N_{ap} are elongated in comparison with the Cu– N_{base} , whereas in the trigonal bipyramids, both Cu– N_{ap} bonds are shorter than Cu– N_{base} .

In studies [17–20], the source of the carbonate group was copper carbonate, CO_2 atmosphere, or air CO_2 . Copper(II) trinuclear complexes were prepared at room temperature, on heating or in conditions of the hydrothermal synthesis starting from copper(II) salts. Magnetic behavior was studied only for two of these compounds: weak antiferromagnetic interactions were found in [Cat](BF_4) $_4 \cdot \text{EtOH} \cdot 3\text{H}_2\text{O}$ [17] and weak ferromagnetic interactions were found in [Cat](CF_3SO_3) $_4 \cdot 0.5\text{H}_2\text{O}$ [20]. It was found that effective magnetic moment μ_{eff} [Cat](BF_4) $_4 \cdot \text{EtOH} \cdot 3\text{H}_2\text{O}$ in the 250–100 K range was 3.3–3.4 μ_{B} , which agrees with spin values for each copper atom $S = 1/2$. To explain the exchange interactions found in [17], the authors used spin Hamiltonian $H = -J_{12}(S_1 \cdot S_2)$, $-J_{13}(S_1 \cdot S_3)$, $-J_{23}(S_2 \cdot S_3)$. The low value of $J = 10.6 \text{ cm}^{-1}$ and weak antiferromagnetic intercluster interactions with $zj = -1.2 \text{ cm}^{-1}$ were explained by large Cu–Cu distances in the Cu_3 cluster (4.64, 4.72, and 5.00 Å). Based on the EPR spectra data for $[\text{Cu}_3(\text{bipy})_6(\mu_3\text{-CO}_3)](\text{CF}_3\text{SO}_3)_4 \cdot 0.5\text{H}_2\text{O}$ [20] with the $\mu_3\text{-}\eta^1\eta^1\eta^1$ -coordination of carbonate ions to copper atoms and the Cu–Cu distances equal to 4.57, 4.68 and 5.19 Å, it was assumed that the magnetic behavior of the complex corresponds to weak ferromagnetic exchange interactions.

The temperature dependence of magnetic susceptibility of a crystalline sample of **1** was measured in the range of 300–2 K. Magnetic moment decreased from 1.98 to 1.33 μ_{B} with the lowering of the temperature. The magnetic moment of three non-interacting copper atoms is $3.4 \pm 0.3 \mu_{\text{B}}$.

Taking into account that the nearest environment of copper atoms Cu(1) and Cu(3) differs from that of Cu(2), as it is found by X-ray diffraction, the magnetic susceptibility of **1** was interpreted using spin Hamiltonian (Fig. 3, insert)

$$H = -2J_1(S_1S_2 + S_2S_3) - 2J_2S_1S_3. \quad (1)$$

Three interacting spin-1/2 particles can form one state with total spin 3/2 and two states with total spin 1/2. Eigen energies of the spin states are $E(3/2) = -J_1 - J_2/2$, $E_1(1/2) = 3J_2/2$, and $E_2(1/2) = 2J_1 - J_2/2$. The magnetic susceptibility of **1** was calculated according to the equation reported in [21]:

$$\chi_M = \frac{N_A g^2 \beta^2}{kT} \times \frac{1/2 \cdot \exp\left(-\frac{E_1(1/2)}{kT}\right) + 1/2 \cdot \exp\left(-\frac{E_2(1/2)}{kT}\right) + 5 \cdot \exp\left(-\frac{E(3/2)}{kT}\right)}{2 \cdot \exp\left(-\frac{E_1(1/2)}{kT}\right) + 2 \cdot \exp\left(-\frac{E_2(1/2)}{kT}\right) + 4 \cdot \exp\left(-\frac{E(3/2)}{kT}\right)}.$$

The best correlation with the experimental data (Fig. 2) is achieved at $2J_1 = 9.8 \pm 0.2 \text{ cm}^{-1}$, $2J_2 = -8.2 \pm 0.2 \text{ cm}^{-1}$, and $g = 2.14 \pm 0.01$. With these parameters of the spin Hamiltonian, the $E(3/2)$ spin state energy is intermediate between the $E_1(1/2)$ and $E_2(1/2)$ energies (Fig. 3b).

The EPR spectrum of **1** was simulated as a sum of spectra of two spin-1/2 complexes and one spin-3/2 complex. Their concentra-

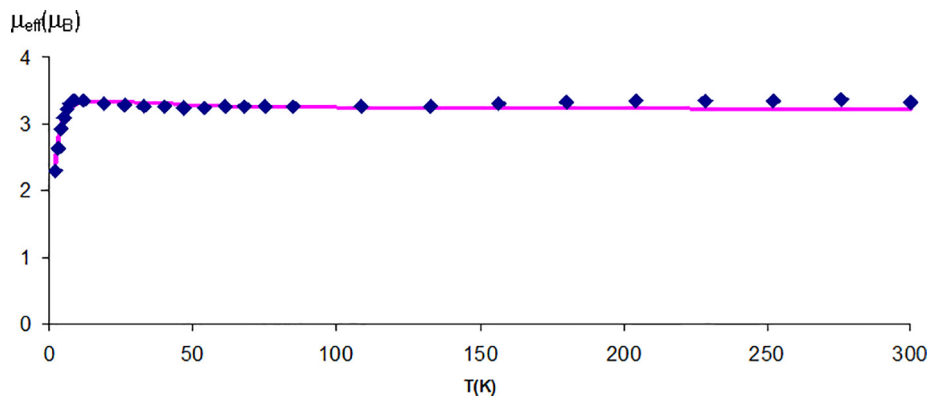


Fig. 2. Temperature dependence of μ_{eff} vs. T (◆); the solid line represents the calculated curve for complex 1.

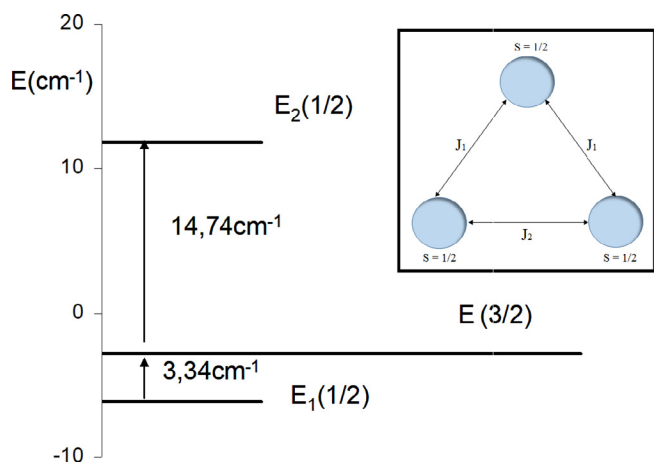


Fig. 3. Geometric model of magnetic exchange in **1**; the insert shows schematic representation of spin state energies in **1** for the best spin Hamiltonian (1) parameters.

tions were calculated according to the Boltzmann occupancies of the corresponding levels.

The spectrum of the spin-3/2 complex is described using the spin Hamiltonian with fine coupling having a rhombic symmetry

$$\hat{H}_{3/2} = \beta(g_x S_x H_x + g_y S_y H_y + g_z S_z H_z) + D(S_z^2 - S(S+1)/3) + E(S_x^2 - S_y^2), \quad (2)$$

where $S = 3/2$ is the total spin; S_z , S_x , and S_y are the projections of the spin operator onto the coordinate axes; D and E are components of the fine coupling tensor; g_x , g_y , and g_z are components of the g tensor; and H is the applied magnetic field. The spectra of two spin-1/2 complexes are simulated by the Zeeman spin Hamiltonian

$$\hat{H}_{1/2} = \beta(g_x S_x H_x + g_y S_y H_y + g_z S_z H_z), \quad (3)$$

where $S = 1/2$ is the total spin of the complex. It was accepted that parameters of two different spin-1/2 complexes are equal.

Computer simulation of the EPR spectrum was performed using the eigenfield method [22]. The D and E parameters and g tensor components are listed in the Table 1.

Table 1

Parameters D and E of spin Hamiltonian (2) and components of the g tensor of spin Hamiltonians (2) and (3) for complex 1.

Spin	C, %	D , cm^{-1}	E , cm^{-1}	g_x	g_y	g_z
1/2	50			2.040	2.080	2.190
3/2	50	0.01767	0.01280	2.030	2.110	2.190

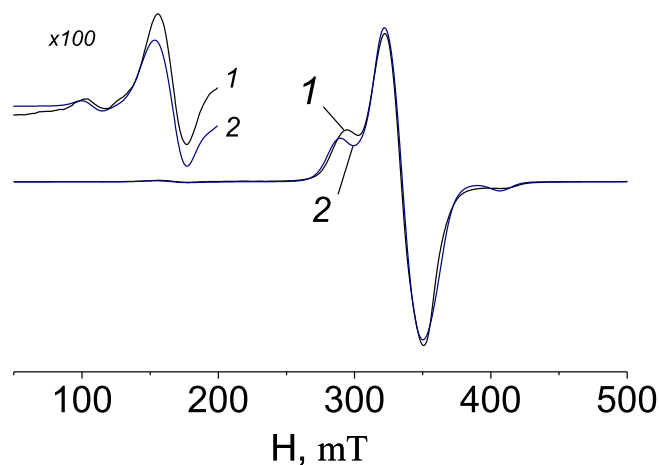


Fig. 4. (1) Experimental and (2) calculated EPR spectrum of a polycrystalline sample of complex **1** at $T = 293$ K.

The complex concentrations in different spin states were calculated from the Gibbs distribution of the corresponding levels taking into account the spin degeneracy. Occupation probability was estimated in accordance with the Boltzmann distribution depending on the energy difference and temperature and spin degeneracy.

A remarkable feature of the EPR spectrum of compound **1** (Fig. 4) is a low-intensity transition in the region of ~ 100 mT in addition to the ordinary “forbidden” transition in the half field (Fig. 5). Formally, it is a $|-3/2\rangle \rightarrow |3/2\rangle$ transition with $\Delta M = \pm 3$. This transition indicates that there exists a state with total spin $S = 3/2$ in the system. The fine coupling tensor admixes the $|-1/2\rangle$ state into the $|3/2\rangle$ state and the $|1/2\rangle$ state into the $|-3/2\rangle$ state making this transition possible [23].

In the earlier papers concerning the structural studies of trinuclear carbonato-bridged copper(II) complexes [17–20], the EPR data are found only for $\text{Cat}(\text{F}_3\text{CSO}_3)_4 \cdot 0.5\text{H}_2\text{O}$ [20]. As it was indicated by the authors, this spectrum contains a very broad signal ($g = 2.13$) and a half-field signal ($g = 4.33$); the spectrum is not present in the paper, and the reported data doesn't allow us to compare the results obtained here with those reported in [20].

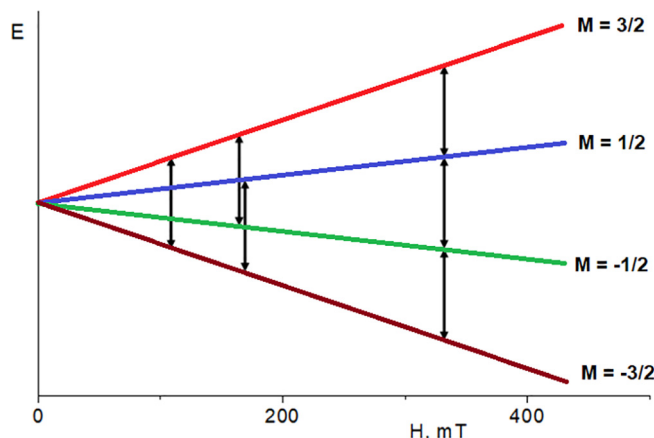


Fig. 5. Schematic representation of energy levels and allowed ($H \sim 300$ mT), “forbidden” ($H \sim 150$ mT), and $\Delta M = \pm 3$ ($H \sim 100$ mT) transitions for the $S = 3/2$ spin under the assumption that $D, E \ll h\nu$.

4. Conclusions

First trinuclear copper(II) complex $[\text{Cu}_3(\text{bipy})_6(\mu_3\text{-CO}_3)] [\text{B}_{12}\text{H}_{12}]_2 \cdot 4.5\text{DMF} \cdot 2\text{H}_2\text{O}$ with the dodecahydro-*closo*-dodecaborate anion has been synthesized and characterized by X-ray diffraction techniques as well as EPR and IR spectroscopic methods. In addition, the DC magnetic susceptibility has been measured. The title compound has been prepared when $[\text{Ag}_2[\text{B}_{12}\text{H}_{12}]]$ is allowed to react with CuCl followed by the addition of bipy in DMF/ CH_3CN . The final product is prepared because of redox reaction $\text{Cu}^+ \rightarrow \text{Cu}^{2+}$ which is accompanied with the isolation of Ag^0 . A number of the B–H...H–C and B–H...H–O shortened contacts have been revealed by the X-ray crystallography. Features of the electronic structure are reported for the trinuclear complex synthesized. In the EPR spectrum, the $\Delta M = \pm 3$ transition is observed indicating the existence of the $S = 3/2$ state of copper. The EPR spectrum is simulated by the spin Hamiltonians for $S = 3/2$ and $S = 1/2$.

Acknowledgments

This study was supported by the Russian Science Foundation (project no. 14-13-01115). The X-ray diffraction studies were performed and described by I.N. Polyakova (deceased) at the Centre of Shared Equipment of the Kurnakov Institute. The EPR studies were performed within the State Assignment on Fundamental Research (no. 0088-2014-0003) to the Kurnakov Institute. The authors thank O.N. Belousova and Dr. L.V. Goeva for the IR spectral studies.

Appendix A. Supplementary data

Supporting Information contains IR spectrum for **1** (Fig. S1), X-ray powder diffraction pattern for **1** (Fig. 2), fragments of the structure and crystal packing (Figs. S3–S8), geometric parameters of hydrogen bonds (Table S1), crystal data and structure refinement (Table S2), and bond lengths and angles (Table S3). Supplementary data associated with this article can be found, in the online version, at <https://doi.org/10.1016/j.ica.2018.04.059>.

References

- [1] E.L. Muetterties, W.H. Knoth, Polyhedral Boranes, Marcel Dekker, New York, 1968.
- [2] N.N. Greenwood, A. Earnshaw, Chemistry of the Elements, second ed., Butterworth-Heinemann, 1997.
- [3] V.V. Avdeeva, E.A. Malinina, I.B. Sivaev, V.I. Bregadze, N.T. Kuznetsov, Crystals 6 (2016) 60.
- [4] V.V. Avdeeva, E.A. Malinina, L.V. Goeva, N.T. Kuznetsov, Russ. J. Inorg. Chem. 55 (2010) 2148–2202.
- [5] V.V. Avdeeva, E.A. Malinina, N.T. Kuznetsov, Russ. J. Inorg. Chem. 62 (2017) 1673–1702.
- [6] V.V. Avdeeva, A.E. Dziova, I.N. Polyakova, L.V. Goeva, E.A. Malinina, N.T. Kuznetsov, Dokl. Chem. 437 (2011) 79–81.
- [7] A.E. Dziova, V.V. Avdeeva, I.N. Polyakova, E.A. Malinina, A.V. Rotov, N.N. Efimov, E.A. Ugolkova, V.V. Minin, N.T. Kuznetsov, Russ. J. Inorg. Chem. 58 (2013) 1527–1535.
- [8] V.V. Avdeeva, A.E. Dziova, I.N. Polyakova, E.A. Malinina, L.V. Goeva, N.T. Kuznetsov, Inorg. Chim. Acta 430 (2015) 74–81.
- [9] V.V. Avdeeva, A.V. Vologzhanina, L.V. Goeva, E.A. Malinina, N.T. Kuznetsov, Inorg. Chim. Acta 428 (2015) 154–162.
- [10] E.A. Malinina, I.K. Kochneva, I.N. Polyakova, V.V. Avdeeva, L.V. Goeva, V.V. Minin, E.A. Ugolkova, N.T. Kuznetsov, Inorg. Chim. Acta 477 (2018) 284–291.
- [11] I.K. Kochneva, I.N. Polyakova, L.V. Goeva, V.V. Avdeeva, E.A. Malinina, N.T. Kuznetsov, Dokl. Chem. 474 (2017) 137–140.
- [12] N.N. Greenwood, J.H. Morris, Proc. Chem. Soc. 11 (1963) 338.
- [13] V.V. Drozdova, E.A. Malinina, O.N. Belousova, I.N. Polyakova, N.T. Kuznetsov, Russ. J. Inorg. Chem. 53 (2008) 1024–1033.
- [14] Yu.V. Rakitin, G.M. Larin, V.V. Minin, Interpretation of EPR Spectra of Coordination Compounds, Nauka, Moscow, 1993 [in Russian].
- [15] G.M. Sheldrick, Acta Crystallogr. A 64 (2008) 112–122.
- [16] C.R. Groom, I.J. Bruno, M.P. Lightfoot, S.C. Ward, Acta Crystallogr. B 72 (2016) 171–179.
- [17] G.A. Albada, I. Matikainen, O.S. Roubeau, U. Turpeinen, J. Reedijk, Eur. J. Inorg. Chem. 14 (2000) 2179–2184.
- [18] W. Huang, P.-Y. Sun, J.-L. Fang, Y.-F. Sun, S.-H. Gou, Transition Met. Chem. 28 (2003) 925–929.
- [19] U.-X. Peng, F. Xu, G. Yin, Q. Lia, W. Huang, J. Coord. Chem. 65 (2012) 3949–3959.
- [20] N. Wannarit, N. Chaichit, C. Pakawatchai, S. Youngme, Russ. J. Inorg. Chem. 36 (2010) 778–785.
- [21] V.T. Kalinnikov, Yu.V. Rakitin, Introduction to Magnetochemistry. Method of Static Magnetic Susceptibility in Chemistry, Nauka, Moscow, 1980 [in Russian].
- [22] G. Belford, R.L. Belford, J.F. Burkhaven, J. Magn. Res. 11 (1973) 251–265.
- [23] A. Abragam, B. Bleaney, Electron Paramagnetic Resonance of Transition Ions, Oxford University Press, Oxford, 1970.